Since January 2020 Elsevier has created a COVID-19 resource centre with free information in English and Mandarin on the novel coronavirus COVID-19. The COVID-19 resource centre is hosted on Elsevier Connect, the company's public news and information website.

Virus Research 176 (2013) 292–297

Contents lists available at SciVerse ScienceDirect

Virus Research

journal homepage: www.elsevier.com/locate/virusres

Short communication

Porcine hemagglutinating encephalomyelitis virus induces apoptosis in a porcine kidney cell line via caspase-dependent pathways

Yungang Lan[a,1], Kui Zhao[a,1], Gaili Wang[a], Bo Dong[a], Jiakuan Zhao[a], Bo Tang[a], Huijun Lu[b], Wei Gao[a], Lingzhu Chang[c], Zhao Jin[a], Feng Gao[a], Wenqi He[a,*]

[a] Key Laboratory of Zoonosis, Ministry of Education, College of Veterinary Medicine, Jilin University, Changchun 130062, China
[b] Key Laboratory of Zoonosis, Ministry of Education, Institute of Zoonosis, Jilin University, Changchun 130062, China
[c] College of Animal Science & Veterinary Medicine, Shenyang Agricultural University, Shenyang 110866, China

ARTICLE INFO

Article history:
Received 19 March 2013
Received in revised form 23 May 2013
Accepted 27 May 2013
Available online 13 June 2013

Keywords:
Procine haemagglutinating encephalomyelitis virus
Apoptosis
PK-15 cells
Caspase

ABSTRACT

Porcine hemagglutinating encephalomyelitis is an acute, highly contagious disease in piglets that is caused by the porcine hemagglutinating encephalomyelitis virus (PHEV). However, the pathogenesis of PHEV and the relationship between PHEV and the host cells are not fully understood. In this study, we investigated whether the PHEV-induced cytopathic effect (CPE) was caused by apoptosis. Replication of PHEV in a porcine kidney-derived cell line (PK-15 cells) caused an extensive CPE, leading to the destruction of the entire monolayer and the death of the infected cells. Staining with Hoechst 33,342 revealed morphological changes in the nuclei and chromatin fragmentation. In addition, PHEV caused DNA fragmentation detectable by agarose gel electrophoresis 48 h post-infection, increasing with the incubation time. The percentage of apoptotic cells increased with the incubation time and reached a maximum at 96 h post-infection, as determined using flow cytometry and fluorescence microscopy of cells that were stained with annexin V-FITC and propidium iodide (PI). Moreover, as is commonly observed for coronavirus infections of other animals, the activities of the effecter caspase, caspase-3, and the initiator caspases, caspase-8 and caspase-9, which are representative factors in the death receptor-mediated apoptotic pathway and the mitochondrial apoptotic pathway, respectively, were increased in PHEV-infected PK-15 cells. Moreover, the tripeptide pan-ICE (caspase) inhibitor Z-VAD-FMK blocked PHEV-induced apoptosis but did not have an effect on virus production by 96 h post-infection. These results suggested that PHEV induces apoptosis in PK-15 cells via a caspase-dependent pathway. Apoptotic death of infected cells is detrimental to animals because it causes cell and tissue destruction. Although the pathological characteristics of PHEV are largely unknown, apoptosis may be the pathological basis of the lesions resulting from PHEV infection.

Porcine hemagglutinating encephalomyelitis virus (PHEV) is a positive, non-segmented, single-stranded RNA coronavirus belonging to betacoronavirus genus within the coronaviridae family, together with mouse hepatitis virus, bovine coronavirus, human coronavirus OC43, human coronavirus HKU1, human coronavirus EMC and severe acute respiratory syndrome coronavirus (Li et al., 2012; Masters, 2006; De Groot et al., 2012). PHEV causes vomiting and wasting disease, and encephalomyelitis in piglets under three weeks old, particularly those lacking PHEV antibodies, such as SPF pigs (Quiroga et al., 2008). Recently, more research has focused on PHEV because infection rates have risen in some countries (Cartwright et al., 1969; Gao et al., 2011; Mengeling and Cutlip, 1976; Quiroga et al., 2008; Rho et al., 2011). This virus spreads to the CNS via peripheral nerves, and nerve cells are one target for viral replication (Hara et al., 2009). In addition, PHEV can be isolated from primary porcine kidney cell cultures (Hirano et al., 1993). Serial propagation of PHEV is feasible in several porcine cell culture systems, e.g., primary pig testis cells, secondary pig thyroid cells as well as swine kidney and swine testis cell lines (Andries and Pensaert, 1980). However, the mechanisms inducing death in PHEV-infected cells remains largely unknown.

Apoptosis is a tightly controlled multistep mechanism of cell death that is characterized by chromatin condensation, plasma-membrane blebbing, cell shrinkage, and DNA fragmentation into membrane-enclosed vesicles or apoptotic bodies (Arends and Wyllie, 1991). The central players in apoptosis are a family of cysteine-dependent proteinases, termed caspases, which catalyze key steps in the death pathway by cleaving substrates at specific

* Corresponding author. Tel.: +86 431 87835376; fax: +86 431 87835376.
E-mail address: hewq@jlu.edu.cn (W. He).
[1] They contributed equally to this work.

0168-1702/$ – see front matter © 2013 Elsevier B.V. All rights reserved.
http://dx.doi.org/10.1016/j.virusres.2013.05.019

sites containing aspartic acid (Cryns and Yuan, 1998). Viruses can trigger apoptosis of infected cells via a range of mechanisms including: receptor binding, activation of protein kinase R (PKR), interaction with p53, expression of viral proteins coupled to MHC proteins on the surface of the infected cell, allowing recognition by cells of the immune system (such as Natural Killer and cytotoxic T cells) that then induce the infected cell to undergo apoptosis (Everett and McFadden, 1999). Apoptosis plays important roles in host protection by eliminating cells damaged by viral infections. Viruses may actively induce apoptosis, consequently facilitating the spread of viral progeny to neighboring cells while limiting host immune/inflammatory responses. However, viruses have evolved strategies to regulate apoptosis, either by blocking a specific step of the cascade or preventing premature death of the host cell, thus maximizing virus production (O'Brien, 1998). Many viruses have the ability to induce apoptosis, which is one of the cytolytic properties of viral infections, and cause a cytopathic effect (CPE) in vitro; these effects are particularly observed in RNA viruses, including coronaviridae (Collins, 2001; Li and Cavanagh, 1992; Liu and Zhang, 2007; Ruggieri et al., 2007; Suzuki et al., 2008). In addition, in some virus-induced diseases, apoptosis is a pathogenic mechanism that contributes to in vivo cell death, tissue injury and disease severity (Clarke et al., 2009; Clarke and Tyler, 2009; Samuel et al., 2007).

In a preliminary investigation, cells of a porcine kidney-derived cell line (PK-15) that were infected with PHEV exhibited distinctive morphological changes and supported PHEV propagation (Lan et al., 2012a,b). In this study, to elucidate the mechanisms of cell injury by PHEV, we investigated whether the PHEV-induced CPE on PK-15 cells was caused by apoptosis by using cytological changes, DNA fragmentation, and caspase activity as indices.

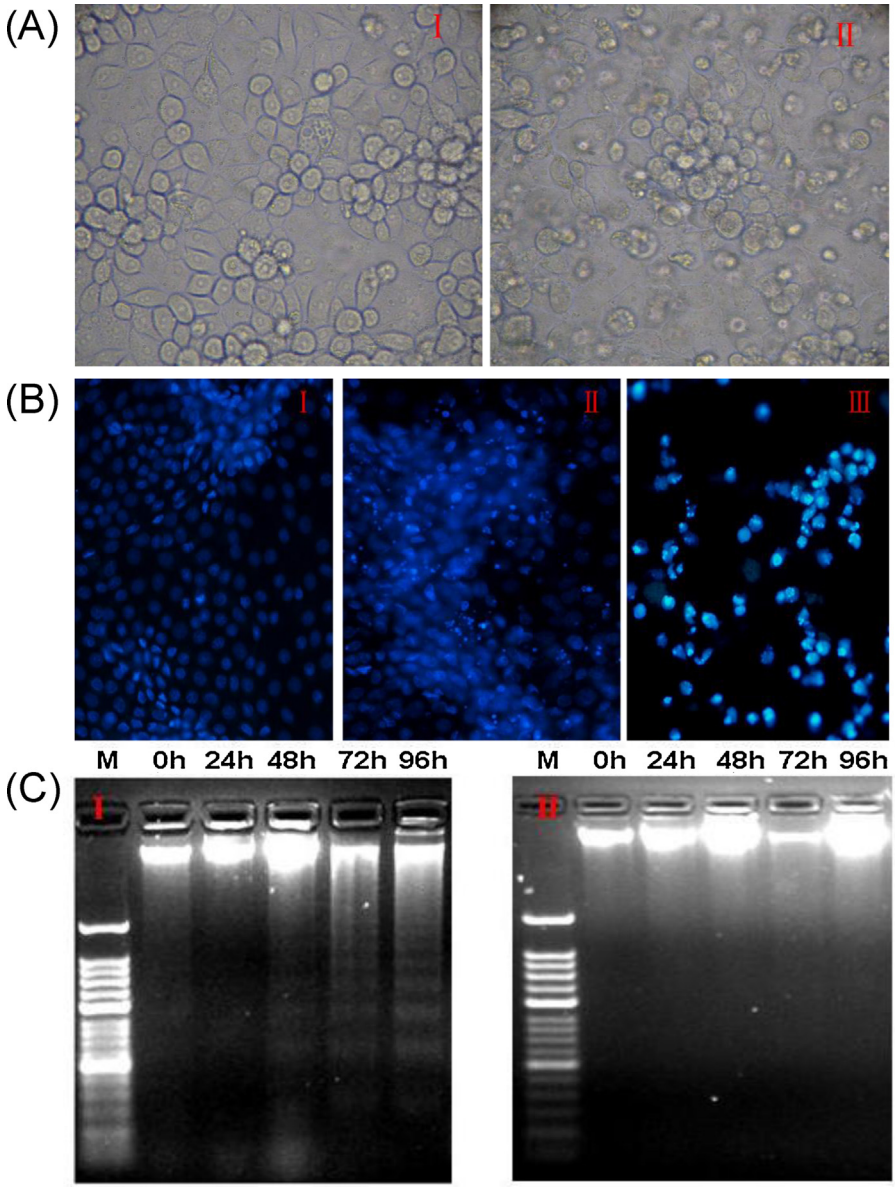

Fig. 1. PHEV induces apoptosis in PK-15 cells. (A) Micrographs of mock-infected and PHEV infected PK-15 cells at 96 h post-infection. In contrast to mock-infected cells (I), PHEV-infected cells exhibit clear signs of shrinkage, rounding and detachment (II). (B) Cells were mock- or PHEV infected, and both adherent and non-adherent cells were isolated at 96 h post-infection, ethanol-fixed, stained with Hoechst 33,342, and viewed using a fluorescence microscope. Hoechst, nuclear staining. I: mock-infected cells, II: adherent infected cells, III: non-adherent infected cells. (C) Agarose gel electrophoresis of the DNA from PHEV-infected cells. DNA fragmentation was observed at and after 48 h post-infection, but was prominent at 72 and 96 h post-infection. I: infected cells M: 50-bp DNA marker, 0–96: 0, 24, 48, 72, and 96 h post-infection, II: mock-infected cells M: 50 bp DNA marker, 0–96: 0, 24, 48, 72, and 96 h post-infection. Cell images were captured at the conclusion of the study. The experiment was performed in triplicate and repeated three times.

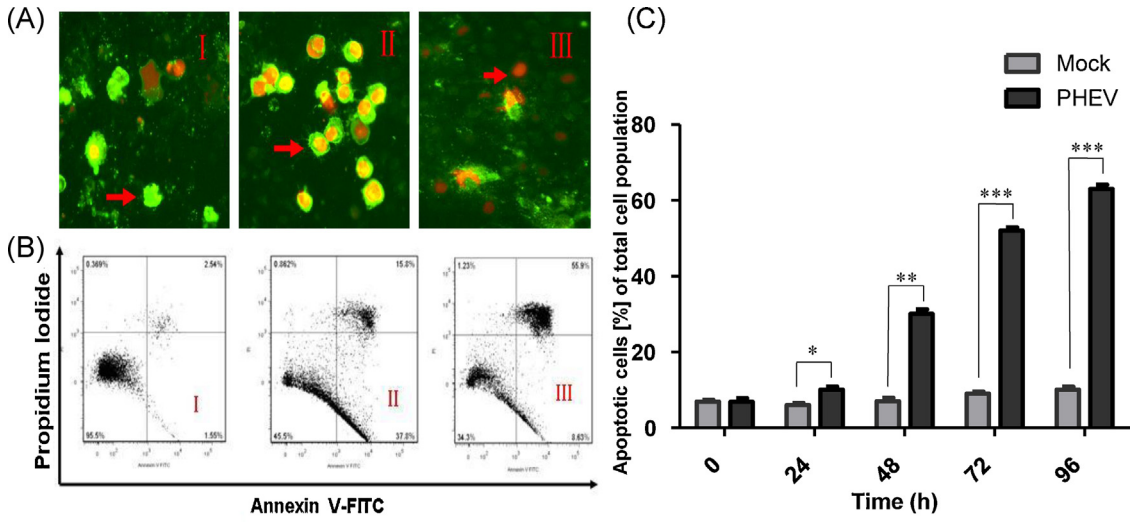

Fig. 2. Apoptotic PHEV-infected PK-15 cells stained with annexin V-FITC/PI were observed by fluorescence microscopy and analyzed by flow cytometry. (A) The samples were analyzed for green fluorescence (FITC) and red fluorescence (PI). Different labeling patterns of the PHEV-infected cells: early apoptotic cells, annexin V-FITC-positive and PI-negative cells (I); necrotic or late apoptotic cells, both annexin V-FITC- and PI-positive (II) cells; dead cells, Annexin V-FITC-negative and PI-positive cells (III). (B) The infected and mock-infected cells were harvested, stained with annexin V-FITC and PI, and analyzed by flow cytometry. Scatter plots of the annexin V-FITC/PI flow cytometry results of a representative experiment are presented below the graphs. The lower right quadrants represent cells in the early stage of apoptosis. The upper right quadrants represent cells in the late stage of apoptosis or necrotic cells. I-III: early and late apoptotic cells at 0, 72, and 96 h post-infection. (C) The data are expressed as the percentage of annexin V-FITC-positive cells (apoptotic cells) at different times. (two-way ANOVA with Bonferroni posttests $^{*}P < 0.05$, $^{**}P < 0.01$,$^{***}P < 0.001$ compared with the data for mock-infected cells).

The PHEV strain used in the current study was HEV-67N (GenBank accession number AY078417) (Mengeling et al., 1972). PK-15 cells [(cultured in MEM supplemented with 10% fetal bovine serum (FBS) and antibiotics (100 μg/ml of streptomycin and 100 U/ml of penicillin)] were seeded in 6-well plates and infected with 400 $TCID_{50}$ ($10^{4.49}$) of PHEV in a 5% CO_2 incubator at 37 °C overnight. Light microscopy of the PHEV-infected PK-15 cells showed that they gradually developed the typical CPE phenotype by 96 h post-infection, including cell rounding and fusion, detachment from the culture dish, and, eventually, cell lysis and death, which was not observed in the mock-infected cells (Lan et al., 2012a,b) (Fig. 1A). The adherent and non-adherent cells were both isolated, ethanol-fixed and treated with 0.2 mg/ml of the membrane permeable DNA-binding dye Hoechst 33,342 for 10 min at 37 °C in dark. Almost all of the non-adherent cells and many of the adherent cells exhibited morphological changes of their nuclei and chromatin fragmentation at 96 h post-infection. However, very few mock-infected cells had detached from the monolayer, and their nuclei were uniformly stained, lacking condensed chromatin (Fig. 1B). In addition, to ascertain whether the induction of apoptosis was correlated with the progression of the CPE, DNA fragmentation, which is a hallmark of cells undergoing apoptosis, was assayed using a previously described method (Herrmann et al., 1994). The cellular DNA from both non-adherent and adherent cells was harvested, and the DNA fragmentation was evaluated. Compared with mock-infected cells, PHEV-infected cells exhibited slight condensation of their chromatin, with heterogeneous nuclear staining patterns appearing between 48 and 72 h post-infection, almost coincident with the appearance of the CPE, and the DNA "ladder" pattern was apparent at 72 and 96 h post-infection (Fig. 1C). These results indicate that PHEV infection may trigger apoptosis in PK-15 cells.

To achieve a better understanding of the pathogenesis of PHEV and the relationship between PHEV and the host cells, the process of PHEV-induced apoptosis in PK-15 cells was assessed by fluorescence microscopy and flow cytometry, as described previously (Chen et al., 2008). Infected and mock-infected cells were harvested by trypsinization and washed twice with cold phosphate-buffered saline (PBS) (0.15 mol/L, pH 7.2). The cells were stained with annexin V-fluorescein isothiocyanate (annexin V-FITC) and propidium iodide (PI) and then examined by fluorescence microscopy to distinguish and quantitatively determine the percentage of dead, viable, apoptotic and necrotic cells after PHEV infection. The different labeling patterns obtained using this assay enabled us to identify the different cell populations: live cells (annexin V-FITC negative/PI negative), early apoptotic cells (intact cell membranes: annexin V-FITC positive/PI negative) (Fig. 2A.I), late apoptotic/necrotic cells (cell membrane not intact: annexin V-FITC positive/PI positive) (Fig. 2A.II) and dead cells (annexin V-FITC negative/PI positive) (Fig. 2A.III). In addition, a flow cytometry was performed using a FACS Canto II flow cytometer (Becton Dickinson, Mountain View, CA, USA) with an excitation of 488 nm. As shown in Fig. 2B and C, the percentage of early apoptotic cells increased with the infection time until reaching a maximum of 37.8% at 72 h post-infection, and the proportion of late apoptotic cells increased from 2.54% at 0 h to 15.9% at 72 h post-infection. A high level of early apoptosis was detected at 72 h post-infection, and a high level of late apoptosis was detected at 96 h post-infection, whereas a basal level of apoptosis and necrosis was observed in the mock-infected control population. Our previous research revealed that the CPE became obvious after 72 h post-infection and that the $TCID_{50}$ reached a maximum at 96 h post-infection, which is consistent with the results obtained in the present study (Lan et al., 2012a,b). Therefore, it seems likely that the CPE of PHEV infection is caused by apoptosis. Further experiments are needed to define the intracellular events that trigger the apoptotic response during PHEV infection.

Caspases are cysteine proteases that play fundamental roles in the apoptotic responses of cells to different stimuli. To gain insight into the mechanism of PHEV-induced apoptosis, the activities of caspase-3, caspase-8, and caspase-9 were determined using caspase-3, -8 and -9 activity assay kits. Briefly, PK-15 cells were collected by trypsinization and rinsed twice with PBS. The lysate was centrifuged for 15 min at 20,000 × *g* at 4 °C. The protein concentration in the supernatants was determined using the Bradford method with bovine serum albumin (BSA) as a standard, and 0.1 mg of total protein was used for each caspase activity assay,

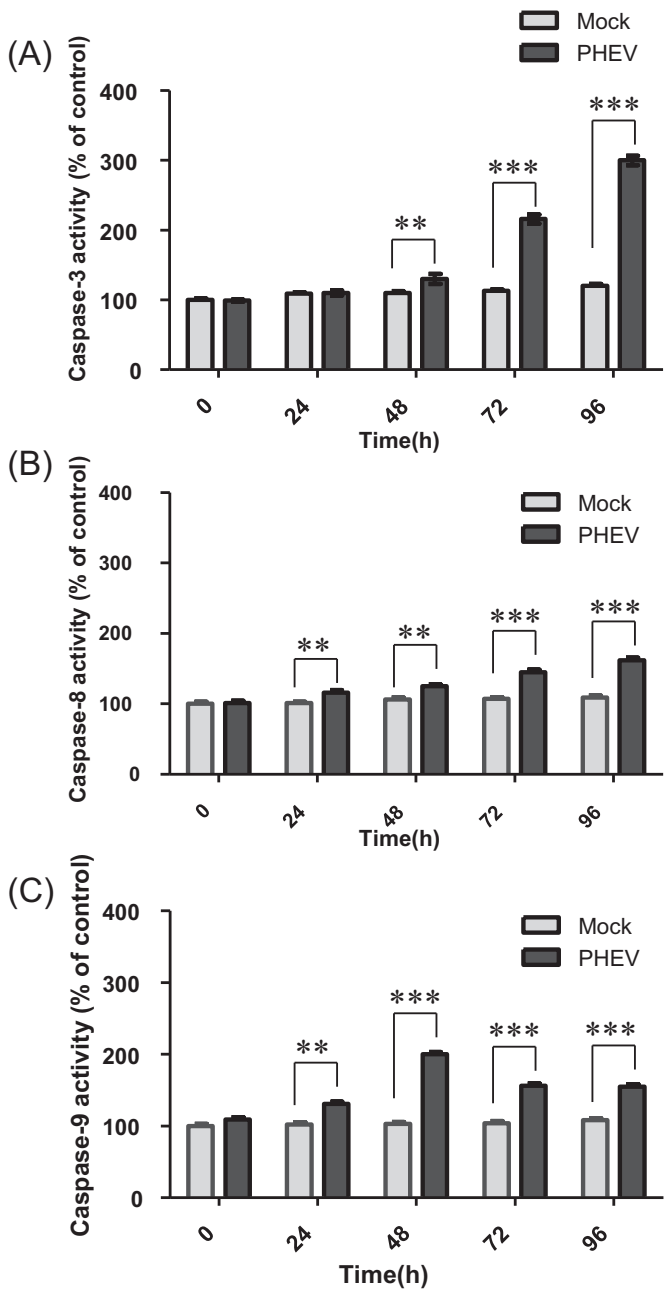

Fig. 3. Kinetics of the activity of caspase-3 (A), caspase-8 (B) and caspase-9 (C) in PHEV-infected (&) and mock-infected (&) cells. Caspase 3, 8 and 9-like protease activity was expressed as the percentage of the activity of mock-infected cells 0 h (control), which was given a value of 100. The data represent the mean values ± SD. (two-way ANOVA with Bonferroni posttests $^{*}P < 0.05$, $^{**}P < 0.01$,$^{***}P < 0.001$ compared with the values for mock-infected cells).

with Ac-DEVD-pNA, Ac-IETD-pNA, and Ac-LEHD-pNA as the substrates for caspase-3, caspase-8, and caspase-9, respectively. Then, the absorbance at 405 nm (OD_{405}) was read using a 96-well plate reader after incubation for 4 h at 37 °C (Wang et al., 2010). An increase in the OD_{405} indicated the activation of caspase-3, -8, and -9.

Caspase-3 is a major effector caspase in both the extrinsic and intrinsic apoptotic pathways acting on enzymes that are indispensable for chromatin condensation and DNA fragmentation (Duprez et al., 2009). Caspase-3 activity was first observed in PHEV-infected cells 48 h post-infection and reached a maximum at 96 h post-infection (Fig. 3A). Based on these results, it was concluded that PHEV infection of PK-15 cells induces apoptosis through activation of the effector caspase, caspase-3. Furthermore, the activities of caspase-8 and caspase-9, which are representative initiator caspases in the death receptor-mediated and mitochondrial apoptotic pathways, respectively, were also measured based on their cleavage of luminogenic substrates. The caspase-8 and caspase-9 activities were increased in PHEV-infected cells at and after 24 h post-infection, and maximal increases were observed at 96 h post-infection and 48 h, respectively, as shown in Fig. 3B and C, (1.6-fold and 2.0-fold increases in activity, respectively, when compared with those of mock-infected cells). These results suggested that PHEV can induce caspase dependent apoptosis in PHEV cells via both the death receptor-mediated and mitochondrial apoptotic pathways. However, the activation of the initiator caspase-8 can also be related to the mitochondrial apoptotic pathway via cleavage of Bid (a member of the proapoptotic Bcl-2 family) and translocation of the truncated Bid to mitochondria (Wang et al., 1996). In some coronaviruses, both initiator caspases are activated in the course of apoptosis; the Fas-signaling pathway in which both initiator caspases are activated via cleavage and translocation of Bid was suggested as the mechanism of apoptosis, particularly in MHV infection(Eleouet et al., 2000; Liu et al., 2006; Liu and Zhang, 2007). Therefore, it was speculated that PHEV also induces apoptosis via a caspase-dependent pathway that may be activated by an interaction between virus protein and cell surface signaling factors with participation of both the death receptor-mediated and mitochondrial apoptotic pathways. However, further investigations that will focus on the kinetics of signal transduction factors are necessary to clarify the detailed mechanisms of PHEV-induced apoptosis.

To determine whether inhibiting apoptosis would abrogate PHEV-induced cell death, PK-15 cells were treated with the general caspase inhibitor, N-benzyloxycarbonyl-Val-Ala-Asp-fluoromethylketone (Z-VAD-FMK) (80 μM) for 2 h prior to, simultaneously with, or 1 h after infection with PHEV at 400 $TCID_{50}$ ($10^{4.49}$). Cells treated with DMSO were used as the controls. To confirm that Z-VAD-FMK inhibited the caspase activity in infected cells, colorimetric assay was performed. The mean optical density (OD_{405}) in case of Z-VAD-FMK treated and infected cells showed significant difference ($^{**}P < 0.01$) from that of PHEV infected alone at 96 h post-infection, and then there was no significant difference among Z-VAD-FMK treated, Z-VAD-FMK treated and infected, DMSO-treated or mock-infected cells suggesting the inhibition of caspase activity in infected cells (Fig. 4A) (Slee et al., 1996). The progress of the infection-induced morphological alterations was monitored by light microscopy. The CPE was delayed in cells that were infected and treated with Z-VAD-FMK, compared to cells that were only infected. The monolayer of cells that were only infected with the virus was destroyed by 96 h post-infection, as expected, whereas at this time, few of the infected and Z-VAD-FMK-treated cells had detached from the monolayer (Fig. 4B). However, the CPE was not completely abolished in the Z-VAD-FMK-treated infected cells; a few rounded cells still attached to the substrate. In addition, PK-15 cells treated as described above were stained with annexin V-FITC and PI and analyzed by flow cytometry. The broad-spectrum pan-caspase inhibitor Z-VAD-FMK significantly protected the PK-15 cells from Z-VAD-FMK-induced apoptosis at 96 h post-infection, resulting in a 40% reduction in the level of apoptotic cells compared to that of untreated infected cells (Fig. 4C). To exclude that this finding was an effect of altered viral replication due to Z-VAD-fmk treatment, virus-titers of PHEV-infected 400 $TCID_{50}$ ($10^{4.49}$) and treated with 0, 25, 50 and 80 μM Z-VAD-fmk were compared. Z-VAD-FMK did not affect the virus titers obtained from PHEV-infected PK-15 cells at 96 h post-infection (Fig. 4D), and hemagglutination assay (HA) was performed to present a kinetics of infection to show that there is no effect of Z-VAD-FMK on viral replication (Vlasak et al., 1988) (data not show). In short, these results

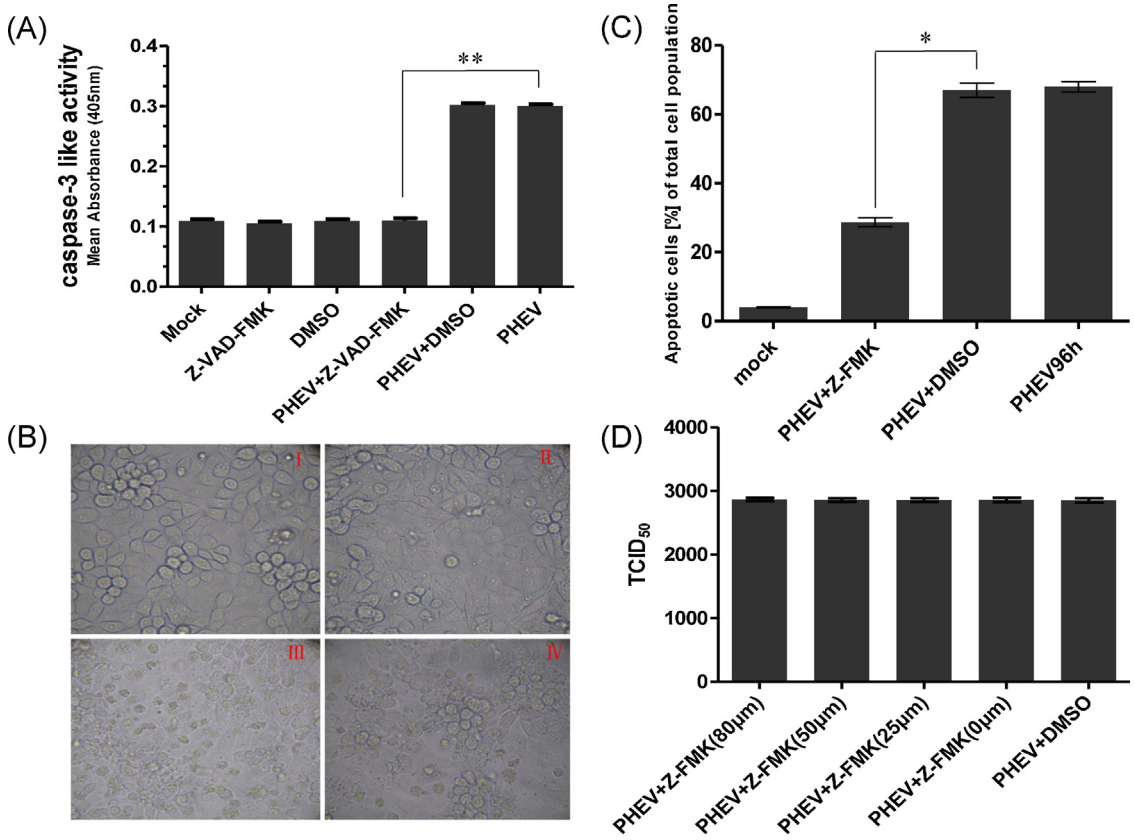

Fig. 4. Effects of Z-VAD-FMK treatment on CPE, cell apoptosis and virus production in PHEV-infected PK-15 cells. (A) The data are expressed as the activity of caspase-3: mock-infected cells (Mock), Z-VAD-FMK treated cells (Z-VAD-FMK), DMSO treated cells (DMSO), cells infected with PHEV alone (PHEV), in the presence of DMSO (PHEV +DMSO) or Z-VAD-FMK (PHEV + Z-FMK-VAD). All determinations were done after 96 h of incubation. The data represent the mean values ± SD (unpaired-samples *t*-test $^{**}P < 0.01$ compared with PHEV-infected cells). (B) Phase-contrast images of mock-infected (I), Z-VAD-FMK treated and infected (II), PHEV-infected (III), DMSO-treated and infected (IV), at an original magnification of 400. The experiment was performed in triplicate and repeated three times. (C) The data are expressed as the percentage of annexin V-FITC-positive (apoptotic cells) cells: mock-infected cells, cells treated with DMSO or Z-VAD-FMK, and cells infected with PHEV after 96 h of incubation (unpaired-samples *t*-test $^{*}P < 0.05$ compared with the DMSO-treated and infected cells). (D) Virus titers at 96 h post-infection of PK-15 cells infected with PHEV alone (PHEV), in the presence of 0, 25, 50 and 80 μM Z-VAD-fmk (PHEV + Z-FMK), or DMSO (PHEV +DMSO).

suggest that PHEV-induced apoptosis may be caspase dependent and apoptosis is not essential for PHEV replication in vitro and mechanisms other than apoptosis may contribute to the overall CPE caused by PHEV replication in PK-15 cells.

In summary, this report demonstrated that PHEV induced apoptosis via a caspase-dependent pathway. However, the detailed mechanisms of caspase activation, more work about will be needed and further investigation using primary porcine cells are needed to clarify the pathobiological characteristics of PHEV, because the findings from this porcine cell line may not faithfully reflect the in vivo situation.

Acknowledgements

This study was supported by the National Natural Science Foundation of China (Nos. 31272530, 31201875, 31172291, and 31072134), the Natural Science Foundation in Jilin Province (No. 201115040), the Graduate Innovation Fund of Jilin University (No. 20121131), and the Fundamental Research Funds of Jilin University.

References

Andries, K., Pensaert, M., 1980. Propagation of hemagglutinating encephalomyelitis virus in porcine cell cultures. Zentralbl Veterinarmed B 27, 280–290.
Arends, M.J., Wyllie, A.H., 1991. Apoptosis: mechanisms and roles in pathology. International Review of Experimental Pathology 32, 223–254.
Cartwright, S.F., Lucas, M., Cavill, J.P., Gush, A.F., Blandford, T.B., 1969. Vomiting and wasting disease of piglets. Veterinary Record 84, 175–176.
Chen, S., Cheng, A.C., Wang, M.S., Peng, X., 2008. Detection of apoptosis induced by new type gosling viral enteritis virus in vitro through fluorescein annexin V-FITC/PI double labeling. World Journal of Gastroenterology 14, 2174–2178.
Clarke, P., Beckham, J.D., Leser, J.S., Hoyt, C.C., Tyler, K.L., 2009. Fas-mediated apoptotic signaling in the mouse brain following reovirus infection. Journal of Virology 83, 6161–6170.
Clarke, P., Tyler, K.L., 2009. Apoptosis in animal models of virus-induced disease. Nature Reviews Microbiology 7, 144–155.
Collins, A.R., 2001. Induction of apoptosis in MRC-5, diploid human fetal lung cells after infection with human coronavirus OC43. Advances in Experimental Medicine and Biology 494, 677–682.
Cryns, V., Yuan, J., 1998. Proteases to die for. Genes & Development 12, 1551–1570.
De Groot, R.J., Baker, S.C., Baric, R., Enjuanes, L., Gorbalenya, A., Holmes, K.V., Perlman, S., Poon, L., Rottier, P.J.M., Talbot, P.J., Woo, P.C.Y., Ziebuhr, J., 2012. Coronaviridae. In: King, A.M.Q., Adams, M.J., Carstens, E.B., Lefkowitz, E.J. (Eds.), Virus taxonomy, classification and nomenclature of viruses, ninth report of the International Committee on Taxonomy of Viruses, International Union of Microbiological Societies, Virology Division. Elsevier Academic Press, Waltham, MA, pp. 806–828.
Duprez, L., Wirawan, E., Vanden Berghe, T., Vandenabeele, P., 2009. Major cell death pathways at a glance. Microbes and Infection 11, 1050–1062.
Eleouet, J.F., Slee, E.A., Saurini, F., Castagne, N., Poncet, D., Garrido, C., Solary, E., Martin, S.J., 2000. The viral nucleocapsid protein of transmissible gastroenteritis coronavirus (TGEV) is cleaved by caspase-6 and -7 during TGEV-induced apoptosis. Journal of Virology 74, 3975–3983.
Everett, H., McFadden, G., 1999. Apoptosis: an innate immune response to virus infection. Trends in Microbiology 7, 160–165.
Gao, W., Zhao, K., Zhao, C., Du, C., Ren, W., Song, D., Lu, H., Chen, K., Li, Z., Lan, Y., Xie, S., He, W., Gao, F., 2011. Vomiting and wasting disease associated with hemagglutinating encephalomyelitis viruses infection in piglets in Jilin, China. Virology Journal 8, 130.
Hara, Y., Hasebe, R., Sunden, Y., Ochiai, K., Honda, E., Sakoda, Y., Umemura, T., 2009. Propagation of swine hemagglutinating encephalomyelitis virus and pseudorabies virus in dorsal root ganglia cells. Journal of Veterinary Medical Science 71, 595–601.

Herrmann, M., Lorenz, H.M., Voll, R., Grunke, M., Woith, W., Kalden, J.R., 1994. A rapid and simple method for the isolation of apoptotic DNA fragments. Nucleic Acids Research 22, 5506–5507.
Hirano, N., Haga, S., Fujiwara, K., 1993. The route of transmission of hemagglutinating encephalomyelitis virus (HEV) 67 N strain in 4-week-old rats. Advances in Experimental Medicine and biology 342, 333–338.
Lan, Y., Lu, H., Zhao, K., He, W., Chen, K., Wang, G., Song, D., Gao, F., 2012a. In vitro inhibition of porcine hemagglutinating encephalomyelitis virus replication with siRNAs targeting the spike glycoprotein and replicase polyprotein genes. Intervirology 55, 53–61.
Lan, Y., Zhao, K., He, W., Wang, G., Lu, H., Song, D., Gao, F., 2012b. Inhibition of porcine hemagglutinating encephalomyelitis virus replication by short hairpin RNAs targeting of the nucleocapsid gene in a porcine kidney cell line. Journal of Virological Methods 179, 414–418.
Li, D., Cavanagh, D., 1992. Coronavirus IBV-induced membrane fusion occurs at near-neutral pH. Archives of Virology 122, 307–316.
Li, Y.C., Bai, W.Z., Hirano, N., Hayashida, T., Taniguchi, T., Sugita, Y., Tohyama, K., Hashikawa, T., 2012. Neurotropic virus tracing suggests a membranous-coating-mediated mechanism for transsynaptic communication. Journal of Comparative Neurology 521, 203–212.
Liu, Y., Pu, Y., Zhang, X., 2006. Role of the mitochondrial signaling pathway in murine coronavirus-induced oligodendrocyte apoptosis. Journal of Virology 80, 395–403.
Liu, Y., Zhang, X., 2007. Murine coronavirus-induced oligodendrocyte apoptosis is mediated through the activation of the Fas signaling pathway. Virology 360, 364–375.
Masters, P.S., 2006. The molecular biology of coronaviruses. Advances in Virus Research 66, 193–292.
Mengeling, W.L., Boothe, A.D., Ritchie, A.E., 1972. Characteristics of a coronavirus (strain 67N) of pigs. American Journal of Veterinary Research 33, 297–308.
Mengeling, W.L., Cutlip, R.C., 1976. Pathogenicity of field isolants of hemagglutinating encephalomyelitis virus for neonatal pigs. Journal of the American Veterinary Medical Association 168, 236–239.
O'Brien, V., 1998. Viruses and apoptosis. Journal of General Virology 79 (Pt 8), 1833–1845.
Quiroga, M.A., Cappuccio, J., Pineyro, P., Basso, W., More, G., Kienast, M., Schonfeld, S., Cancer, J.L., Arauz, S., Pintos, M.E., Nanni, M., Machuca, M., Hirano, N., Perfumo, C.J., 2008. Hemagglutinating encephalomyelitis coronavirus infection in pigs, Argentina. Emerging Infectious Diseases 14, 484–486.
Rho, S., Moon, H.J., Park, S.J., Kim, H.K., Keum, H.O., Han, J.Y., Van Nguyen, G., Park, B.K., 2011. Detection and genetic analysis of porcine hemagglutinating encephalomyelitis virus in South Korea. Virus Genes 42, 90–96.
Ruggieri, A., Di Trani, L., Gatto, I., Franco, M., Vignolo, E., Bedini, B., Elia, G., Buonavoglia, C., 2007. Canine coronavirus induces apoptosis in cultured cells. Veterinary Microbiology 121, 64–72.
Samuel, M.A., Morrey, J.D., Diamond, M.S., 2007. Caspase 3-dependent cell death of neurons contributes to the pathogenesis of West Nile virus encephalitis. Journal of Virology 81, 2614–2623.
Slee, E.A., Zhu, H., Chow, S.C., MacFarlane, M., Nicholson, D.W., Cohen, G.M., 1996. Benzyloxycarbonyl-Val-Ala-Asp (OMe) fluoromethylketone (Z-VAD.FMK) inhibits apoptosis by blocking the processing of CPP32. Biochemical Journal 315 (Pt 1), 21–24.
Suzuki, K., Matsui, Y., Miura, Y., Sentsui, H., 2008. Equine coronavirus induces apoptosis in cultured cells. Veterinary Microbiology 129, 390–395.
Vlasak, R., Luytjes, W., Leider, J., Spaan, W., Palese, P., 1988. The E3 protein of bovine coronavirus is a receptor-destroying enzyme with acetylesterase activity. Journal of Virology 62, 4686–4690.
Wang, C.J., Hu, C.P., Xu, K.P., Yuan, Q., Li, F.S., Zou, H., Tan, G.S., Li, Y.J., 2010. Protective effect of selaginellin on glutamate-induced cytotoxicity and apoptosis in differentiated PC12 cells. Naunyn-Schmiedeberg's Archives of Pharmacology 381, 73–81.
Wang, K., Yin, X.M., Chao, D.T., Milliman, C.L., Korsmeyer, S.J., 1996. BID: a novel BH3 domain-only death agonist. Genes & Development 10, 2859–2869.